



Revue Paralia, Volume 6 (2013) pp 9.61-9.90

Keywords: Suspended sediment transport, Vertical distribution of the concentration, Nonequilibrium profile, Deposition, Erosion, Rouse-Vanoni profile. © Editions Paralia CFL

Nonequilibrium description of the vertical distribution of the suspended sediment transported by open surface flows, considering erosion and deposition phenomena

Martin SANCHEZ¹

1. Université de Nantes, Faculté des Sciences et des Techniques,
UMR-6112 du CNRS - Planétologie et Géodynamique, 2 rue de la Houssinière,
BP 92208, 44322 Nantes cedex 3, France. *martin.sanchez@univ-nantes.fr*

Abstract:

This study is based on data obtained from the numerical solution of a 1DV theoretical transport equation. These data have been used to implement a model describing the vertical profile of the suspended matter concentration, in connexion with problems of sediment transport by open surface flows.

For an unsteady state, without erosion or deposition, a first description of the vertical concentration distribution is proposed. This is similar to the general equation of the steady state concentration profile and involves a parameter named alpha, which always tends towards its terminal theoretical value corresponding to the steady state.

With deposition or erosion, if the variables of the problem remain constant, and the solid exchanges between the bed and the flow are proportional to the sediment settling velocity multiplied by the bottom concentration, it is observed in this study that the concentration profile tends towards a terminal shape. In accordance with the approach adopted, a modification of the shape of the concentration profile is linked to the solid exchanges at the bottom. This modification is described by a function to which a second parameter, called beta, is added.

The entire model for the vertical profile of the concentration in unsteady state with erosion and deposition, involves two non-dimensional parameters, alpha and beta, and a dimensional parameter, which is the reference concentration. A stationarity of alpha and beta parameters is possible with erosion or deposition, implying necessarily a non stationarity of the reference concentration.

Time-variations of non-dimensional parameters of the model are described by two phenomenological equations. A good adjustment of all the proposed formulations allows to obtain a very stable and accurate model, which can be used to improve the precision of results obtained from 2DH transport models.

*Received 2 October 2013, accepted 28 October 2013, available online 6 November 2013.
Translated version not certified, published under the responsibility of the article author.*

How to cite the original paper:

SANCHEZ M. (2013). *Description non stationnaire de la distribution verticale des sédiments transportés en suspension par les écoulements à surface libre, en présence de dépôt et d'érosion*. Revue Paralia, Vol. 6, pp 9.1–9.30.

DOI:10.5150/revue-paralia.2013.009

(disponible en ligne – <http://www.paralia.fr> – available online)

1. Introduction

With today's computers, and a moderate calculation cost, the 2DH hydrodynamic models used in ocean, coastal, lake, estuarine and river environments, allow the applications at a fine scale covering large areas and over long periods.

When the variables studied by these models can be properly described as a function of the vertical coordinate, the results obtained are very similar to those from three-dimensional models. Two successful applications following this approach are: (i) models of wave propagations above a slightly inclined bottom describing the vertical distribution of the velocity potential with Stokes-Airy's theory, and, (ii) models of homogeneous fluid streams that integrate shear stress over the full depth to take into account its effect on vertical mean velocities.

One of the aims of this paper is to include, in 2DH modelling of suspended sediment transport by open surface flows, an accurate description of the vertical distribution of the sediment. Beyond the Rouse-Vanoni law, which is valid for uniform and steady states, the developed model can be applied in unsteady and non-uniform conditions, when the solid exchanges at the bottom are parameterized by a deposition or erosion rate. With this model, the reference bottom concentration can be known in order to properly calculate the rate of deposition. This model also allows to know at any time the vertical distribution of the suspended matters, for all practical purposes.

2. Theory

In the problems studied in this paper, fine sediments in suspension are transported by currents with their horizontal velocity. In a 3D turbulent flow, the instantaneous local value of the suspended matter concentration c fluctuates around a mean value C . The decomposition of c is written as follows:

$$c = C + c' \quad (1)$$

where c' is the fluctuation of the concentration. If molecular mass diffusion is neglected, the concentration C in a turbulent flow is governed by the following transport equation (Cartesian coordinate system $Oxyz$ with z as the vertical coordinate):

$$\frac{\partial C}{\partial t} + V_x \frac{\partial C}{\partial x} + V_y \frac{\partial C}{\partial y} + V_z \frac{\partial C}{\partial z} = -\frac{\partial \langle v_x' c' \rangle}{\partial x} - \frac{\partial \langle v_y' c' \rangle}{\partial y} - \frac{\partial \langle v_z' c' \rangle}{\partial z} + \frac{\partial (W C)}{\partial z} \quad (2)$$

where W is the local mean value of the suspended sediment settling velocity, V_x , V_y and V_z are the local components of the velocity characterizing the mean turbulent flow, and terms $\langle v_x' c' \rangle$, $\langle v_y' c' \rangle$, $\langle v_z' c' \rangle$, represent the temporal correlations between fluctuant velocity components and the fluctuation of the concentration. The latter quantify mass transfers linked to the turbulence. Usually, these terms are modeled as follows by the Fick-Boussinesq diffusion law:

$$\langle v_x' c' \rangle = -K_x \frac{\partial C}{\partial x} \quad , \quad \langle v_y' c' \rangle = -K_y \frac{\partial C}{\partial y} \quad , \quad \langle v_z' c' \rangle = -K_z \frac{\partial C}{\partial z} \quad (3)$$

where K_x , K_y and K_z are turbulent diffusion coefficients in the x , y and z directions, respectively. The 3D transport equation becomes:

$$\frac{\partial C}{\partial t} + V_x \frac{\partial C}{\partial x} + V_y \frac{\partial C}{\partial y} + V_z \frac{\partial C}{\partial z} = \frac{\partial}{\partial x} \left(K_x \frac{\partial C}{\partial x} \right) + \frac{\partial}{\partial y} \left(K_y \frac{\partial C}{\partial y} \right) + \frac{\partial}{\partial z} \left(K_z \frac{\partial C}{\partial z} \right) + \frac{\partial(WC)}{\partial z} \quad (4)$$

The solution of this equation must satisfy a border condition concerning the sediment exchanges at the bottom.

If the bottom is located at $z=0$, in the case of resuspension described by an effective erosion rate E^{ef} (sediment source term in $\text{kg m}^{-2} \text{s}^{-1}$), the border condition is:

$$\left(-WC - K_z \frac{\partial C}{\partial z} \right) \Big|_{z=0} = E^{ef} \quad (5)$$

In case of deposition, the border condition is:

$$\left(-WC - K_z \frac{\partial C}{\partial z} \right) \Big|_{z=0} = -D^{ef} \quad (6)$$

where D^{ef} denotes the effective deposition rate (sediment sink term in $\text{kg m}^{-2} \text{s}^{-1}$), which can be calculated by the following formulation (KRONE, 1986; METHA, 1986):

$$D^{ef} = p W_0 C_0 \quad (7)$$

where, on the one hand, C_0 is the suspended sediment concentration at the bottom of the flow and W_0 the mean settling velocity of this suspended sediment. On the other hand, the term p represents, according to KRONE (1986), the probability [0;1] of the bottom settling sediments to adhere to the bed. If $p=0$, all the particles touching the bed are immediately resuspended by the flow and the effective deposition rate is zero.

If the sedimentary regime is steady and uniform, the problem is greatly simplified and the vertical distribution of C is governed by:

$$WC = -K_z \frac{\partial C}{\partial z} \quad (8)$$

Integration of this equation allows to obtain the Rouse-Vanoni generalized law for a steady state of the suspended matter vertical distribution (ORTON & KINEKE, 2001; SANCHEZ *et al.*, 2005):

$$C(z) \Big|_{steady-state} = C_0 \exp \left(- \int_0^z \frac{W}{K_z} dz \right) \quad (9)$$

The above equation can be analytically resolved depending on the expressions of K_z and W . Some known solutions are presented in the appendices 1 at the end of this paper. In what follows, these two physical magnitudes are considered to be invariants with z . The expression 9 becomes:

$$C(z^\circ) \Big|_{steady-state} = C_0 \exp(-P^e z^\circ) \quad (10)$$

where $z^\circ = z/d$ is the non dimensional vertical coordinate, d the depth and P^e the Peclet number characterizing the vertical sediment convection-diffusion transfers:

$$P^e = \frac{W d}{K_z} \quad (11)$$

One usual relation to evaluate K_z is:

$$K_z = \frac{\kappa}{6} U_c d \quad (12)$$

where U_c is the shear velocity and $\kappa=0.4$ the universal Karman constant.

The expression of C_0/\bar{C} ratio (where \bar{C} is the mean concentration over all the depth) is obtained by integrating the equation 10:

$$\left. \frac{C_0}{\bar{C}} \right|_{steady-state} = \frac{P^e}{1 - \exp(-P^e)} \quad (13)$$

Equation 13 could be used in 2DH modelling to estimate the bottom concentration C_0 as a function of the mean vertical concentration \bar{C} . Actually the knowledge of C_0 is needed to reliably estimate the rate of deposition by equation 7.

Nevertheless, in accordance with the numerical simulations carried out by TEETER (1986), results obtained from hydro-sedimentary modelling show that when the sedimentation of suspended sediment begins to occur, the C_0/\bar{C} ratio decreases compared to the value given by equation 13. This decrease is explained by a reduction of the concentration, which is relatively important near the bottom as shown in Figure 1. A formulation from TEETER (1986) which allows the calculation of C_0/\bar{C} ratio in current existing models (LUMBORG & WINDELIN, 2003) is written as follows:

$$\frac{C_0}{\bar{C}} \approx 1 + \frac{P^e}{1.25 + 4.75 p^{2.5}} \quad (14)$$

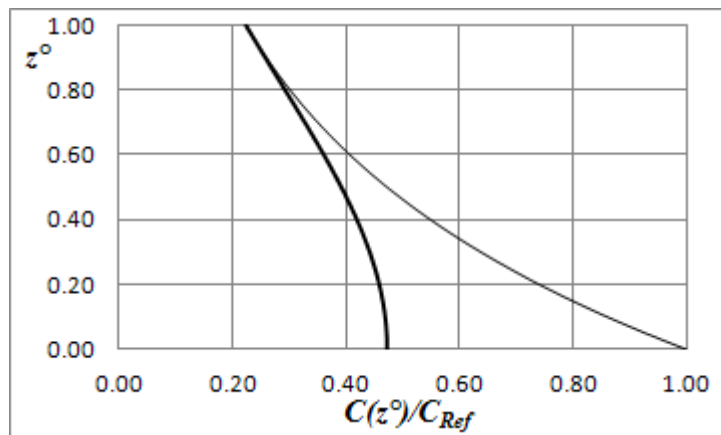


Figure 1. Illustration of the sedimentation effects on the concentration vertical profile.
Thin line: steady state law. Thick line: profile observed during a deposition period
($z^o=0$ =bottom; $z^o=1$ =surface).

Studies on non-cohesive sediment transport show that when the Peclet number exceeds a critical threshold P_{cr}^e , whose value is between 9 and 15, transport in suspension cannot occur (TEETER, 1986). This criterion should be applicable also for fine sediments when the value of the Peclet number remains below the critical value long enough compared to the time required for suspended particles to settle.

3. Methods

In order to understand the dynamic behaviour of sediments in the water column, a 1DV numerical model based on the following equation has been implemented:

$$\frac{\partial C}{\partial t} = \frac{\partial}{\partial z} \left(\frac{\kappa}{6} U_c d \frac{\partial C}{\partial z} + WC \right) \quad (15)$$

Tests have been carried out for a wide range of values of the problem variables covering most possible real cases of fine sediment transports by coastal and estuarine flows. During these tests, different values of the studied variables were combined. Among the values examined are:

- 8 values of d (in m): 0.25; 0.5; 1; 2; 4; 8; 16 and 32.
- 6 values of W (in mm s^{-1}): 0.05; 0.1; 0.2; 0.4; 0.8 and 1.6.
- Values of U_c (in m s^{-1}) variables ranging between 0.00002 and 0.3.

The numerical models discretize the water column in N layers of constant non-dimensional thickness equal to $\Delta z^{\circ} = \Delta z/d = 1/N$. In most tests the value of N was fixed at 50, but in some specific tests $N=100$ was retained. At every modelling step, and in every instant t , the concentration C_i is known in the middle of each layer i of the water column whose non-dimensional level measured from the bottom is $z_{i-1/2}^{\circ} = (i-1/2)\Delta z^{\circ}$.

3.1 Unsteady state without erosion or deposition

The first tests were carried out with a cyclical variation of the shear velocity given by the following expression:

$$U_c = U_{c-moy} [1 + \text{Ampl} \times \cos(\omega t)] \quad (16)$$

where U_{c-moy} is the mean shear velocity of the test, Ampl is a parameter defining the relative amplitude of the oscillation of U_c , and $\omega = 2\pi/T$ is the angular frequency which is linked to the oscillation period T .

In most tests, the parameter Ampl was fixed at 0.80 (except in a reduced number of cases for which the retained value is mentioned), and the period T at 22320 s, which is half of the theoretical value of the semidiurnal tide period. For the parameter U_{c-moy} (in m s^{-1}), the following four values have, in particular, been studied: 0.01; 0.02; 0.04 and 0.08.

3.1.1 Description of the vertical concentration profile without erosion or deposition

Initial tests have shown that the vertical concentration profile remained, in most cases, close to the decreasing exponential law. Nevertheless, it should be indicated that these profiles are not exactly in accordance with that law. In order to adjust at every modelling time t , an exponential equation for the concentrations profile, the least square method was used.

In accordance with this method, if a variable Y is linearly linked to a variable X , and $\hat{Y} = A + BX$ is the best approach of Y adjusted in agreement with this criterion, then the A and B parameters are given by:

$$A = \frac{N \sum_{i=1}^N X_i Y_i - \sum_{i=1}^N X_i \sum_{i=1}^N Y_i}{N \sum_{i=1}^N X_i^2 - \left(\sum_{i=1}^N X_i \right)^2} \quad (17)$$

$$B = \frac{\sum_{i=1}^N X_i^2 \sum_{i=1}^N Y_i - \sum_{i=1}^N X_i Y_i \sum_{i=1}^N X_i}{N \sum_{i=1}^N X_i^2 - \left(\sum_{i=1}^N X_i \right)^2} \quad (18)$$

where X_i and Y_i are the associated pairs of the experimental values of these variables and N the total number of these pairs.

If the vertical profile of the concentration is approached by the following equation:

$$\hat{C}(z^\circ) = \hat{c} \exp(-\hat{\alpha} z^\circ) \quad (19)$$

where \hat{c} is a reference concentration and $\hat{\alpha}$ is a parameter, then, the problem is linearized, making the following change of variables: $X_i = z^\circ_i$ and $Y_i = \ln(C_i)$. In this case, the adjusted parameters are given by: $\hat{\alpha} = -A$ and $\hat{c} = \exp(B)$.

3.1.2 Characterizing the error between the adjusted exponential law and the vertical profile of the concentration resulting from 1DV model

The relative error associated with the estimation of C_i by \hat{C} , is defined as follows:

$$\hat{e}(z^\circ) = \frac{\hat{C}(z^\circ) - C_i(z^\circ)}{C_i(z^\circ)} \quad (20)$$

At every step of the 1DV numerical modelling, the function $\hat{e}(z^\circ)$ can be evaluated from results of $C_i(z^\circ)$ and by using the adjusted values of the parameters \hat{c} and $\hat{\alpha}$ to compute $\hat{C}(z^\circ)$.

3.2 Unsteady state with erosion and deposition

Tests of the 1DV numerical model with deposition and/or erosion were made by combining the different values of the problem parameters given above.

Tests of depositions were realized with the following values of parameter p of Krone's sedimentation law (Equation 7): 0.125, 0.25, 0.5 and 1.

To characterize erosion tests, a non dimensional erosion rate q was defined as follows:

$$q = \frac{E^{ef}}{W_0 C_0} \quad (21)$$

The studied parameter q values are: 0.125; 0.25; 0.5; 1; 2; 4; 8 and 16.

A reduced number of tests were carried out with a fixed value of the $E^{ef}/(W_{init} \times C_{init})$ ratio, where W_{init} and C_{init} are the initial values (at $t=0$) of the variables W and C , respectively.

4. Results from numerical 1DV simulations and development of a phenomenological model

4.1 Sedimentary transport without erosion or deposition

4.1.1 Relative local error linked to the adjusted exponential law describing the vertical profile of the concentration

The analysed tests correspond to a variation of U_c according to equation 16, for different values of the magnitudes U_{c-moy} , W and d .

The study of function $\hat{e}(z^\circ)$ characterizing the relative local error associated with the estimation of C_i , by the \hat{C} adjusted equation, shows that in all the cases $\hat{e}(z^\circ)$ profiles remain similar (Figure 2). Maximum value of $|\hat{e}|$ is always observed at the bottom (at $z^\circ=0$). The sign of \hat{e} at the surface is always opposite to the one corresponding to the bottom. The vertical profile of the relative error includes systematically 3 crossings passing by $\hat{e}=0$. Although the level z° of these crossings varies slightly from one case to another, the following values can be mentioned:

- Superior crossing: $z^\circ \approx 0.90$
- Intermediate crossing: $z^\circ \approx 0.51$
- Inferior crossing: $z^\circ \approx 0.12$

The study of the relative error allows to draw figure 3, with 51840 values of $\hat{e}(z^\circ=0)$, combining different values of the problem variables.

In 90% of the studied cases, the absolute value of $\hat{e}(z^\circ=0)$ remains less than 0.03, and in 99%, less than 0.23. However, in some cases, the maximum values of $|\hat{e}(z^\circ=0)|$ exceeds a value of 0.40. It was found that the highest errors correspond to larger Peclet numbers, which reach a value of 12 in these tests. It should be noted that the values of Peclet numbers are greater than the critical threshold P_{cr}^e above which a transport by suspension cannot occur, involving a deposition of the suspended sediment that is not taken into account in this first series of modelling.

A very close relationship was found between the instantaneous values $\hat{e}(z^{\circ}=0)$ and some characteristic parameters of the problem (see Figure 3). The following law was adjusted (it overestimates the error for great values of $d\hat{\alpha}/dt$):

$$\hat{e}(0)_{estim} \approx -0.108 \frac{d}{U_c} \frac{d\hat{\alpha}}{dt} \quad (22)$$

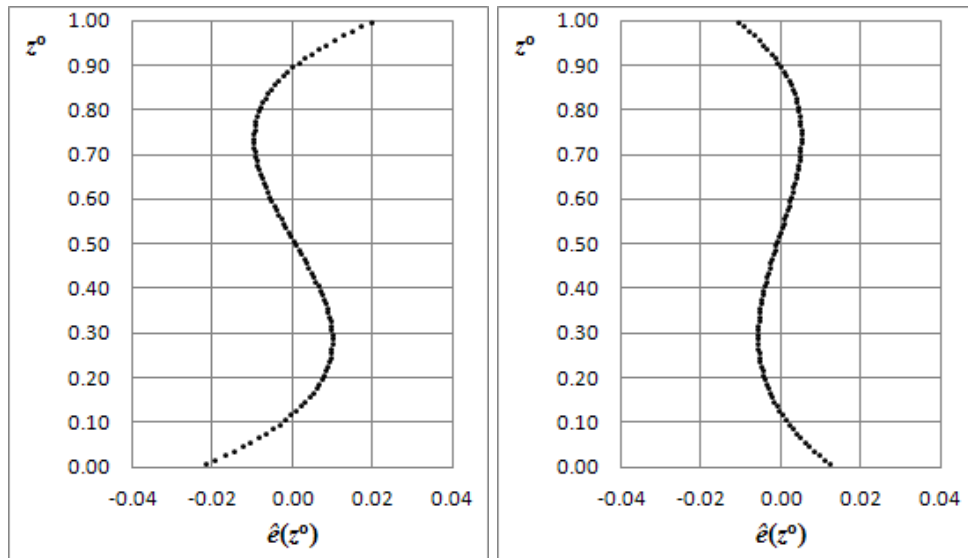


Figure 2. Examples of two $\hat{e}(z^{\circ})$ vertical profiles corresponding to maximum errors observed for the test defined by: $U_{c-moy}=0.02 \text{ m s}^{-1}$; $W = 0.0002 \text{ m s}^{-1}$ and $d = 8 \text{ m}$.

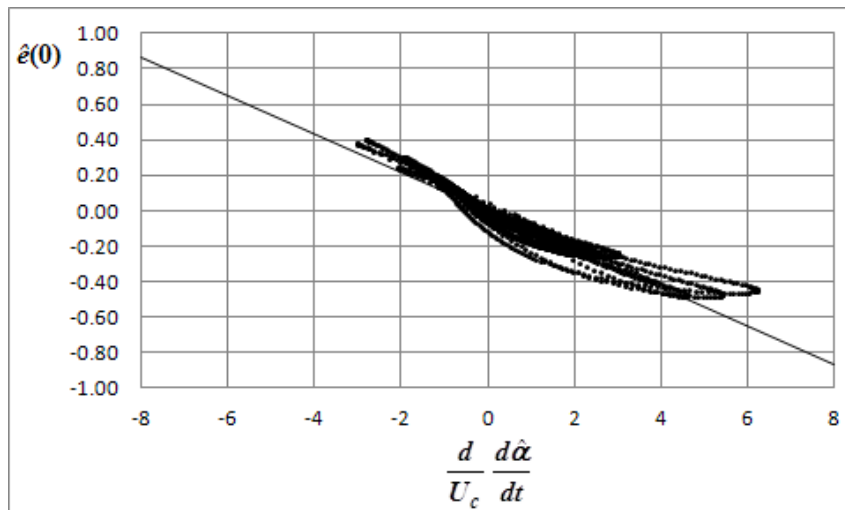


Figure 3. Relation between $\hat{e}(z^{\circ}=0)$ and $(d/U_c) \times d\hat{\alpha}/dt$ according to the IDV numerical modelling (the figure contains 51840 experimental points).

Due to the high correlation coefficient justifying equation 22, it could be included in a model to improve its accuracy. However, knowing that the extreme values of $\hat{e}(z^{\circ}=0)$

are observed for well-marked conditions of deposition, this option is not considered as the study of sediment transport without deposition or erosion has little interest.

It must be noted that a positive value of $d\hat{\alpha}/dt$, which corresponds to a period of concentration increasing at the bottom and decreasing at the surface, is accompanied by a negative value of $\hat{e}(0)$. This indicates that near the bed, the value of \hat{C} , according to the adjusted law, is lower than the concentration C_i evaluated with 1DV model.

4.1.2 Modelling of the vertical concentration profile in unsteady state without deposition or erosion

After confirming that, in similarity with equation 10 and 19, the C/C_0 ratio can be modelled correctly by a function $F(z^\circ; \alpha) = \exp(-\alpha z^\circ)$, a phenomenological model is used to describe the vertical profile of the concentrations of unsteady state without deposit or erosion. This is written as follows:

$$\tilde{C}(z^\circ) = \tilde{c} \exp(-\tilde{\alpha} z^\circ) \quad (23)$$

where \tilde{c} is the reference concentration near the bed and $\tilde{\alpha}$ is the model parameter (the smaller the parameter $\tilde{\alpha}$, the more uniform the vertical distribution of sediment).

Plots of $\hat{\alpha}$ and P^e as a function of time show that in all the cases studied the signal $\hat{\alpha}(t)$ is lagging behind $P^e(t)$. At every instant t , $\hat{\alpha}$ value tends towards P^e value (Figure 4). It was also found that the maximum and minimum in signal $\hat{\alpha}(t)$ corresponded to the moment when the two signals crossed. Finally, the analysis shows that the phase shift depends mainly on the U_c/d ratio. On the basis of these observations the retained model to simulate the variation in time of $\tilde{\alpha}$ is the following:

$$\frac{d\tilde{\alpha}}{dt} = c_\alpha \frac{U_c}{d} (\alpha_\infty - \tilde{\alpha}) \quad (24)$$

where $\alpha_\infty = P^e$ is the terminal steady state value of the parameter $\tilde{\alpha}$ and c_α a coefficient of the model. All the numerical results from 1DV model were used to validate the above equation and to evaluate $c_\alpha \approx 0.667$.

An equivalent expression to equation 23 was used by BELINSKY *et al.* (2005) to study the load of a water column with depth $d \rightarrow \infty$, caused by an erosion of the bed. By assuming the existence of a terminal saturation value for C_0 , they obtained a model somewhat different from that defined by equation 24.

Figure 4 is an example of results for a test case. This figure shows the time variations of: (i) U_c (in dm s^{-1}), (ii) P^e , (iii) parameter $\hat{\alpha}$ evaluated from the results of 1DV model adjusted according to the least square method, and (iv) parameter $\tilde{\alpha}$ obtained from equation 24 resolved numerically using the *predictor-corrector* method of Runge-Kutta. In addition, this figure shows $\hat{e}(z^\circ=0)$ evaluated from numerical simulations on one hand and estimated with the empirical approach defined by Eq. 22 on the other hand.

The most important phase shift between the signals $P^e(t)$ and $\hat{\alpha}(t)$ were observed for $d=32$ m and $U_{c\text{-moy}}=0.01$ m s^{-1} , which are the maximum and minimum values studied for

these two magnitudes. The curves of Figure 5 correspond to this case. As a consequence of the high value of the d/U_c ratio, maximum values observed of $\hat{e}(z^0=0)$ are here very high, and always associated with extreme values of P^e .

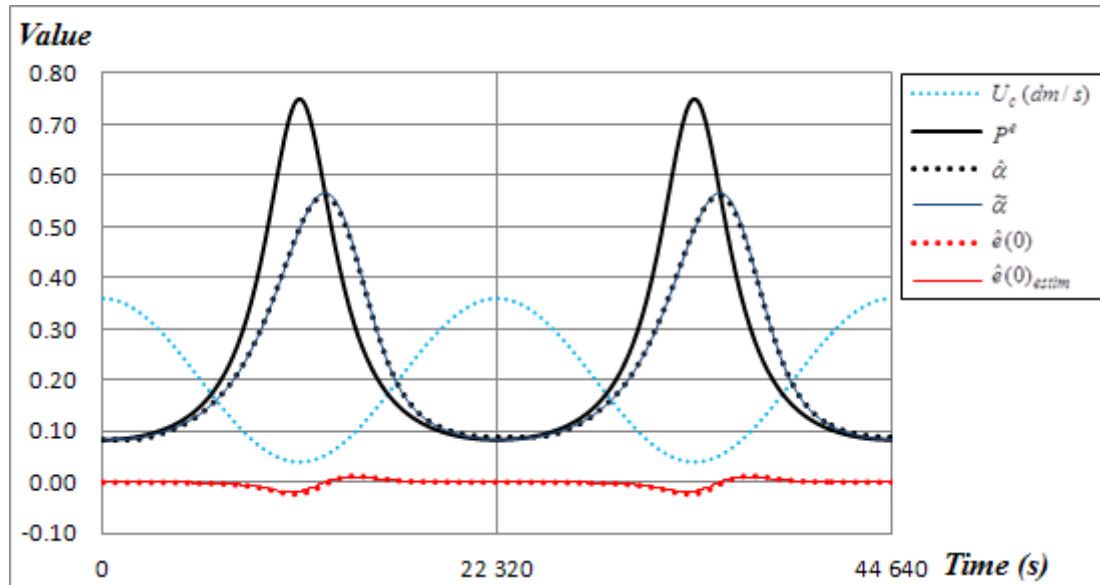


Figure 4. Results validating the phenomenological model in unsteady state, without erosion or deposition, corresponding to the test-case defined by:
 $U_{c-moy}=0.02 \text{ m s}^{-1}$; $W = 0.0002 \text{ m s}^{-1}$ and $d = 8 \text{ m}$.

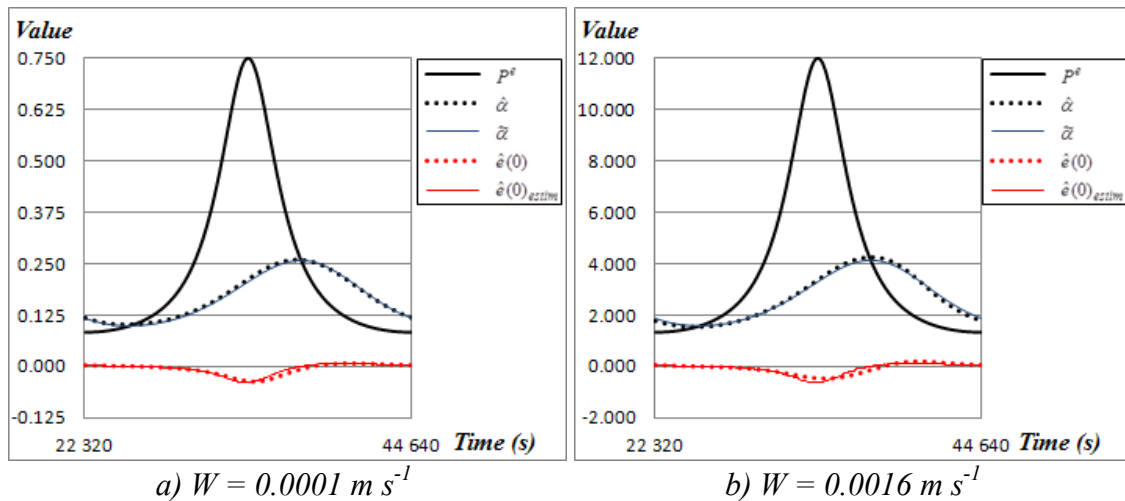


Figure 5. Results for unsteady state, without erosion or deposition, corresponding to two test-cases defined by: $U_{c-moy}=0.01 \text{ m s}^{-1}$ and $d = 32 \text{ m}$.

Figure 5a corresponds to a settling velocity $W=0.0001 \text{ m s}^{-1}$ and Figure 5b to $W=0.0016 \text{ m s}^{-1}$. Between these two cases the $\hat{\alpha}(t)/P^e$ ratios remain nearly identical, but with a small difference involving a slight dependence of the c_α coefficient of the

phenomenological model with regards to the value of $\hat{\alpha}$ when it becomes high, and have the same order of magnitude as P^e_{cr} . This dependence is neglected in this study in the range of values examined for the variables of the problem.

For values U_{c-moy}/d greater than about 0.02, the phase shift between the signals $P^e(t)$ and $\hat{\alpha}(t)$ is negligible, except in the temporal neighbourhood of the maximum of the Peclet number (Figure 6).

In fact, in a coastal environment, the maximum for the Peclet number is observed when the direction of the tidal stream reverses, so that U_c can tend towards zero. Thus, sedimentary regime can be considered steady during part of a tidal cycle and unsteady during the complementary part. Insofar as the U_c signal considered in the modelling has a period $T=22320$ s (which is representative of the semidiurnal tides with a period of 44640 s), the following criterion to determine whether the sediment regime in a given environment is steady or unsteady at any moment can be proposed:

$$\text{If : } \frac{U_c \times T}{d} > \sim 500, \text{ the sedimentary regime is nearly steady} \quad (25)$$

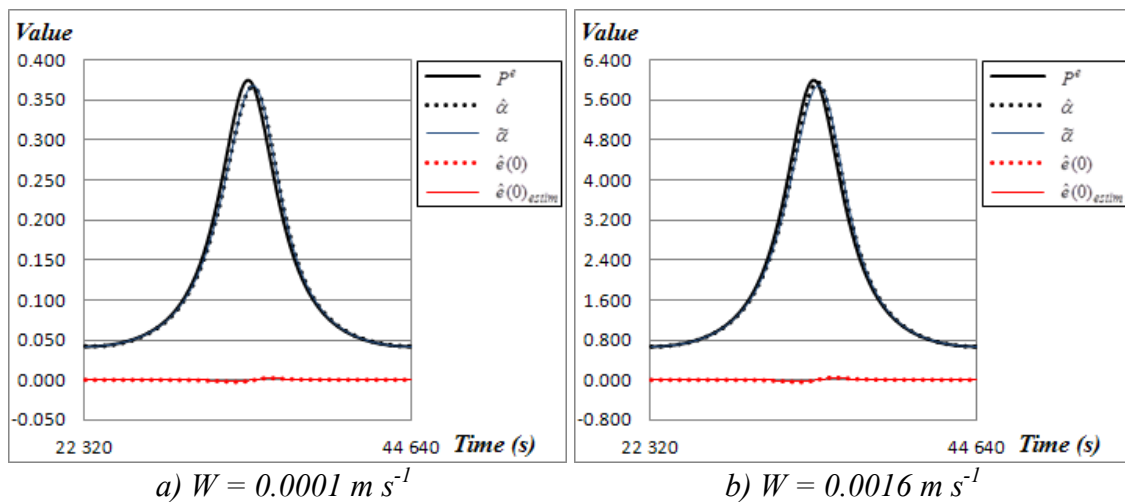


Figure 6. Results for unsteady state, without erosion or deposition, corresponding to two test-cases defined by: $U_{c-moy}=0.02 \text{ m s}^{-1}$ and $d = 1 \text{ m}$.

In order to explore the robustness of the phenomenological model, some tests were carried out including values of $U_c \rightarrow 0$ for which $P^e \rightarrow \infty$. These tests correspond to a settling velocity $W=0.0002 \text{ m s}^{-1}$ and a variation of the shear velocity controlled by $U_{c-moy}=0.02 \text{ m s}^{-1}$ and $Ampl=0.999$, so that during the modelling the minimum value of U_c is of $2 \times 10^{-5} \text{ m s}^{-1}$ and the associated maximum Peclet number is equal to 150. The corresponding results, represented in Figure 7, show the validity of the phenomenological model for this extreme case.

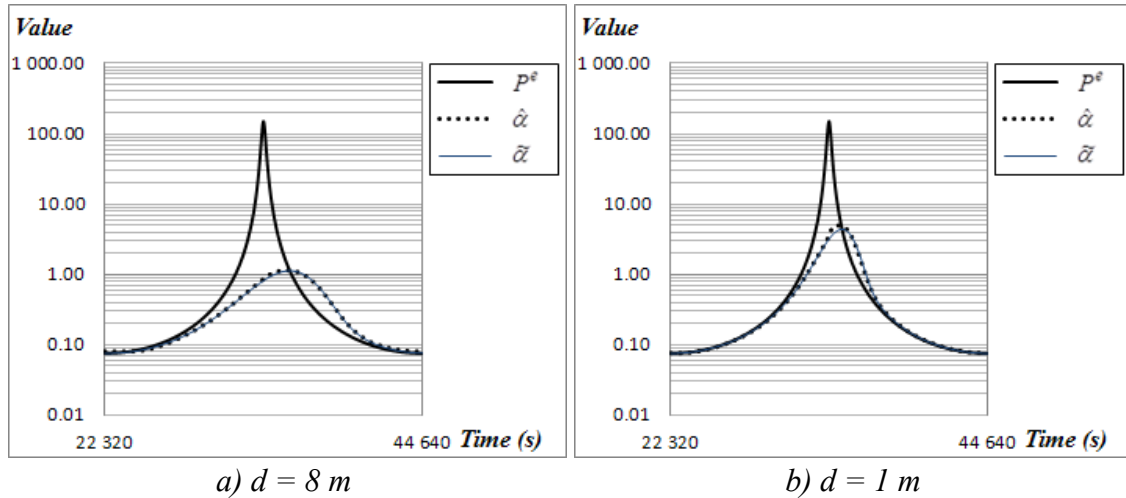


Figure 7. Results for unsteady state, without erosion or deposition, corresponding to two test-cases defined by: $W=0.0002 \text{ m s}^{-1}$, $U_{c\text{-moy}}=0.02 \text{ m s}^{-1}$ and $Ampl=0.999$.

These results also confirm that the c_α coefficient of the phenomenological model is dependent on the value of $\hat{\alpha}$. In fact, it seems that for great values of $\hat{\alpha}$ the coefficient c_α increases slightly. This dependence is neglected in this study.

The phenomenological model for variation of $\tilde{\alpha}$ remains stable for $U_c=0$, because in this extreme case equation 24 becomes:

$$\frac{d\tilde{\alpha}}{dt} = c_\alpha \left(\frac{6W}{\kappa d} \right), \text{ if } : U_c = 0 \quad (26)$$

Although for $U_c=0$ the model is stable, it should be noted that during the period of time when this condition persists, the sediments settle without turbulent mixing, so that the actual shape of the suspended vertical solid profiles deviates from that of an exponential law, and even more so that this period of time is long.

As a consequence of the no deposition condition imposed, which is unrealistic for $U_c=0$, sediments tend, according to the 1DV modelling results, to accumulate in the lower layers of the water column, which is accompanied, in accordance with equation 26, by an increase in the estimated values for the parameter $\tilde{\alpha}$.

4.2 Sedimentary transport with erosion and/or deposition

Modifications induced on the vertical profile of the suspended sediment concentration by deposition and erosion phenomena are generally greater than that due to the non stationarity of the sediment regime linked exclusively with the fluctuations of the hydrosedimentary variables. The effects of these two exchanges of sediments between the bed and the flow are described thereafter.

4.2.1 Description of the vertical profile of the concentrations in unsteady state with deposition

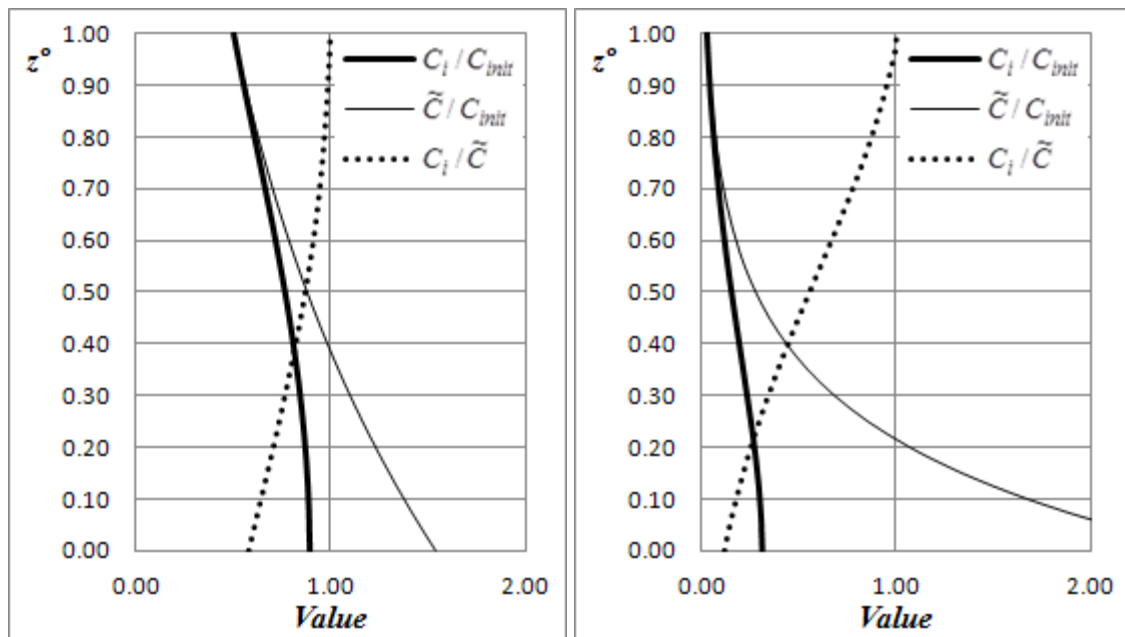
Research work for a description of the vertical profile of the concentration in unsteady state with deposition is based on results of 1DV numerical model combining the different values examined for magnitudes U_{c-moy} , W and d .

The examined tests were carried out for the following values of the parameter p of Krone's sedimentation law (equation 7): 0.125; 0.25; 0.5 and 1.

The first part of this work examines the properties of the $C_i(z^\circ)/\tilde{C}(z^\circ)$ ratio, where C_i defines the concentration obtained from 1DV numerical model for unsteady state with deposition (Figure 8). It was observed that in most cases this ratio can be described by an exponential law as: $G(z^\circ; \beta) = \exp(-\beta(1-z^\circ)^2)$. For this reason, the retained phenomenological model to describe the concentration is written as follows:

$$C(z^\circ) = C_R \exp(-\alpha z^\circ) \exp(-\beta(1-z^\circ)^2) \quad (27)$$

Where C_R is a reference concentration and β a parameter of the model depending on the variable of the problem. The objective with this model is to minimize the difference between $C(z^\circ)$ and $C_i(z^\circ)$, as much as possible.



a) $P^e=0.98$; $p=1$; $d=8$ m; $W=0.0004$ m s⁻¹

b) $P^e=3.9$; $p=1$; $d=8$ m; $W=0.0016$ m s⁻¹

Figure 8. Examples of vertical profiles of $C_i(z^\circ)/\tilde{C}(z^\circ)$ ratio, evaluated from 1DV model results with deposition (for C_i) and from the phenomenological model adjusted in unsteady state, without erosion or deposition (for \tilde{C}).

Given that $\alpha = \tilde{\alpha}$ was retained, the experimental value of the reference concentration is calculated as follows as a function of the value of the surface concentration issued from the 1DV numerical model:

$$C_R = \frac{C_{i=N+1/2}(z^\circ = 1)}{\exp(-\alpha)} = \frac{1.5 C_{i=N} - 0.5 C_{i=N-1}}{\exp(-\alpha)} \quad (28)$$

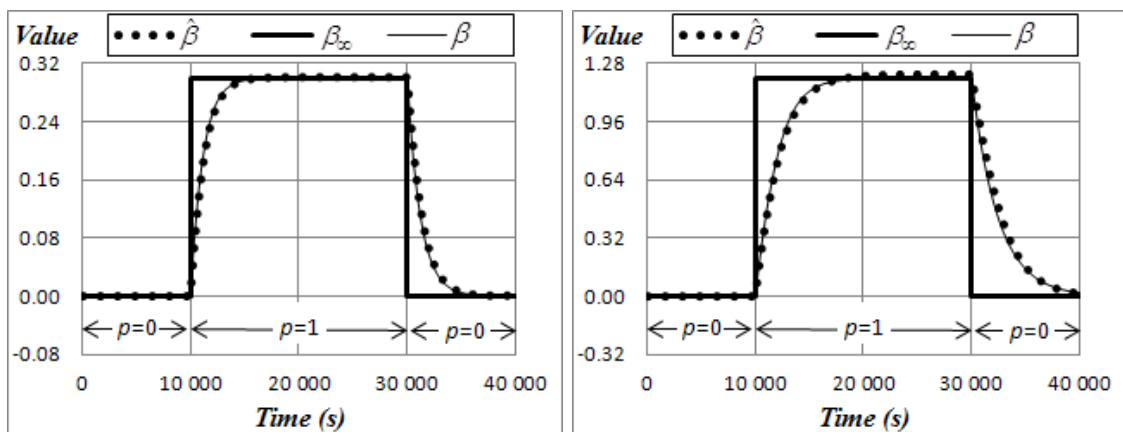
The theoretical values of $G_i(z^\circ)$ are determined by:

$$G_i(z^\circ) = \frac{C_i(z^\circ)}{C_R \exp(-\alpha z^\circ)} \quad (29)$$

Finally, the experimental value of $\hat{\beta}$ was obtained by an adjustment of the data to function $\hat{G}(z^\circ) = \exp(-\hat{\beta}(1-z^\circ)^2)$ in accordance with the least square criterion:

$$\hat{\beta} = \frac{\sum_{i=1}^N (1-z_i^\circ)^2 \ln(G_i)}{\sum_{i=1}^N (1-z_i^\circ)^4} \quad (30)$$

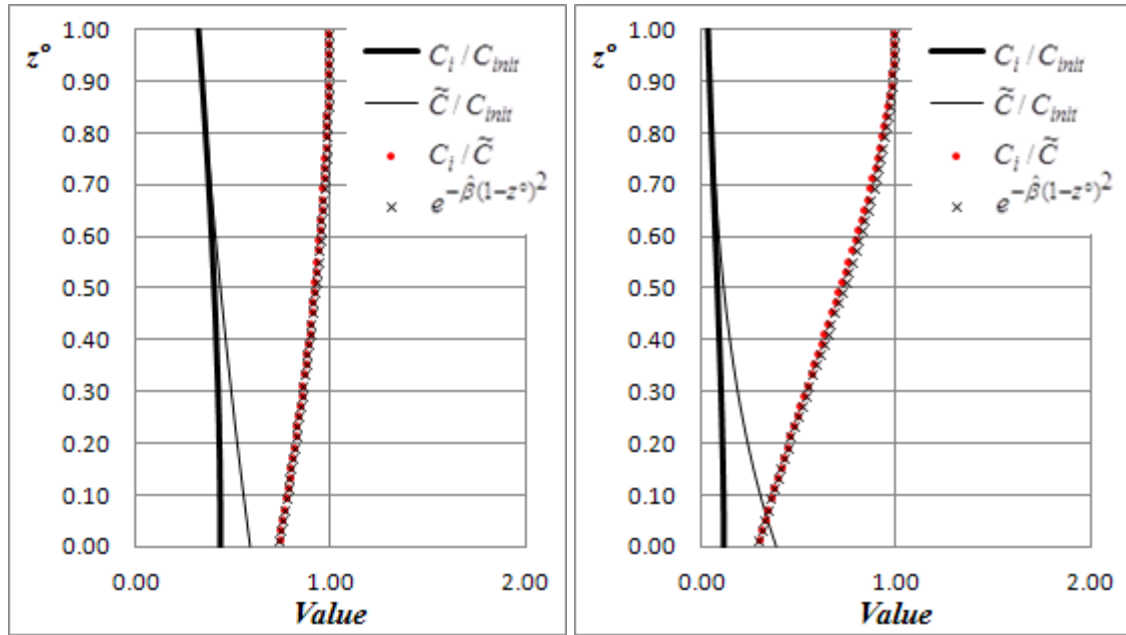
It was found that a stationary terminal value β_∞ can be determined for parameter $\hat{\beta}$ if the independent variables of the problem (U_c , W and d) remain constant, provided that parameter p of Krone's sedimentation law (Equation 7) is also constant. Under these conditions, deposition processes cause a gradual decrease in suspended matter concentrations, but stationarity is observed for parameter $\hat{\beta}$. The simulations using the 1DV numerical model regarding deposition conditions imposed by steps, show that in all cases the value of $\hat{\beta}$ tends to a terminal value β_∞ (see Figures 9 and 10).



a) $\alpha=Pe=0.6$; $W=0.0004 \text{ m s}^{-1}$; $d=8 \text{ m}$

b) $\alpha=Pe=2.4$; $W=0.0008 \text{ m s}^{-1}$; $d=8 \text{ m}$

Figure 9. Results from 1DV numerical tests in unsteady state with deposition represented by values of $\hat{\beta}$. Evolution of $\beta_\infty=0.5 p\alpha$, according to its adjusted law, and variation of β according to the phenomenological model defined by equation (31) resolved by the predictor-corrector method of Runge-Kutta.



a) $\alpha = P^e = 0.6; p = 1; W = 0.0004 \text{ m s}^{-1}; d = 8 \text{ m}$

b) $\alpha = P^e = 2.4; p = 1; W = 0.0008 \text{ m s}^{-1}; d = 8 \text{ m}$

Figure 10. Results from 1DV numerical tests in unsteady state with deposition represented by an instantaneous profile of C_i/C_{init} . Instantaneous profile of \tilde{C}/C_{init} according to the phenomenological model without erosion or deposition. Ratio C_i/\tilde{C} and function $\hat{G}(z^o) = \exp(-\hat{\beta}(1-z^o)^2)$ adjusted from this ratio.

Simulations with deposition by steps were realized as a function of the variables of the problem to assess terminal values of β_∞ corresponding to a steady state of parameter $\hat{\beta}$. Figure 11 shows that β_∞ can be linked to parameters p and α by: $\beta_\infty = 0.5 p \alpha$. In the same way as for parameter $\tilde{\alpha}$, results show that the phase shift between $\beta(t)$ and $\beta_\infty(t)$ signals depends mainly on the U_c/d ratio. Based on this observation, the retained mode to simulate the time variations of β is:

$$\frac{d\beta}{dt} = c_\beta \frac{U_c}{d} (\beta_\infty - \beta) \quad (31)$$

where c_β is a model coefficient whose value is estimated from the curves of $\hat{\beta}(t)$ issued from numerical 1DV tests with deposition imposed by steps (see Figure 9). Assessment of this coefficient leads to writing:

$$c_\beta = \begin{cases} 0.667 + 0.3 \times \beta & , \text{ if } D^{ef} > 0 \\ 0.667 & , \text{ if } D^{ef} = 0 \end{cases} \quad (32)$$

It is interesting to notice that for a steady terminal regime of α and β parameters, the phenomenological model implemented in this article can be written as follows:

$$C(z^o)|_{\alpha_\infty, \beta_\infty(p, \alpha)} \approx C_R \exp(-P^e z^o) \exp(-0.5 p P^e (1-z^o)^2) \quad (33)$$

So, this approach of the vertical profile of the concentrations is compatible with the border conditions at the bottom and the surface. In fact we can get:

$$\left(-W C|_{\alpha_{\infty}, \beta_{\infty}(p, \alpha)} - K_z \frac{\partial C|_{\alpha_{\infty}, \beta_{\infty}(p, \alpha)}}{\partial z} \right)_{z=0} = \left(-p W C|_{\alpha_{\infty}, \beta_{\infty}(p, \alpha)} \right)_{z=0} \quad (34a)$$

$$\left(-W C|_{\alpha_{\infty}, \beta_{\infty}(p, \alpha)} - K_z \frac{\partial C|_{\alpha_{\infty}, \beta_{\infty}(p, \alpha)}}{\partial z} \right)_{z=d} = 0 \quad (34b)$$

However, it should be noted that when parameters α and β are not in a steady state, these boundary conditions are not strictly fulfilled, so that in these cases the model includes uncertainty that can be studied through the inherent errors associated to the results of the phenomenological model. The study of these errors will be made in 4.2.3, where deposition and erosion are simulated during the same test.

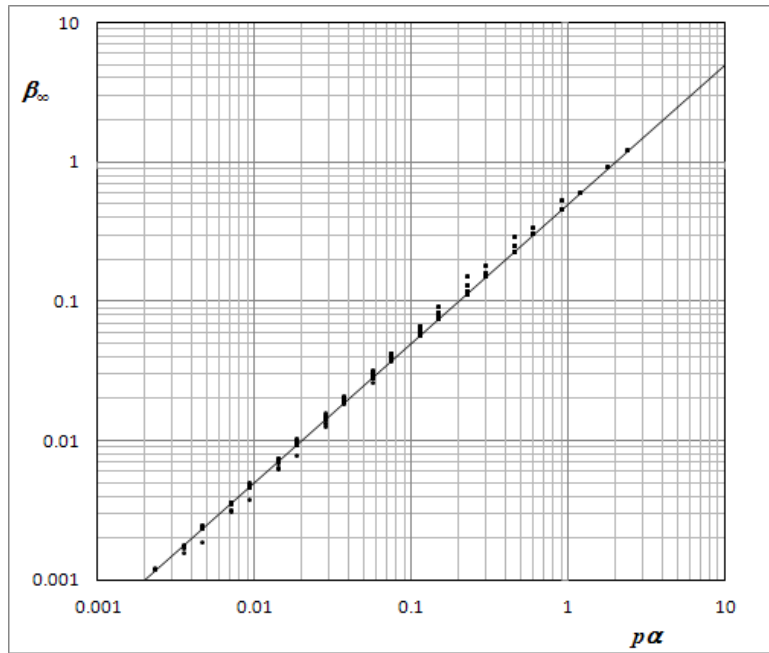


Figure 11. Parameter β_{∞} as a function of $p \times \alpha$ (516 experimental points).
The continuous line corresponds to the adjusted law $\beta_{\infty} = 0.5 p \alpha$.

4.2.2 Description of the vertical profile of the concentrations in unsteady state with erosion

Parameter β taking into account the effect of depositions on the vertical profile of concentrations can also be used to consider erosion effects. As for the deposition case, it is observed that a stationary terminal value of β_{∞} can be determined for parameter $\hat{\beta}$ if the independent variables of the problem (U_c , W and d) remain constant, but only if a parameter defined by $q = E^{ef} / (C_0 W_0)$ remains also constant.

It should be noted that this last condition is not "natural" in sedimentary processes because generally E^{ef} is considered to be independent of C_0W_0 . Indeed, it is recognized that the effective erosion rate E^{ef} depends mainly on the erosive hydrodynamic stresses and the resistance of sediments towards these stresses. However, modelling of erosion by steps with invariant q parameter provides the most accurate numerical method available to assess β_∞ and c_β (see Figures 12 and 13). Tests allowed to evaluate $c_\beta=0.667$.

In terminal steady state for parameters α and β , a relationship $\beta_\infty=-0.5\times q\alpha$ is compatible with the border conditions at the bottom and surface. The results of the 1DV numerical erosion imposed by steps show that this relationship is only valid for values of q less than 0.1 (see Figure 14), although above this value β_∞ is closely correlated with $q\alpha$. The retained approach is:

$$\beta_\infty = \begin{cases} -0.50 \times (q\alpha) & , \text{if : } q\alpha < 0.10 \\ -0.72 \times (q\alpha)^{1.15} & , \text{if : } q\alpha > 0.10 \end{cases} \quad (35)$$

We must point out that in the course of this study we found that in some cases, particularly with erosion, the results from 1DV numerical model with $N=20$ are less accurate than those from the phenomenological model developed in this paper. In this study, this problem was resolved taking $N=50$, or $N=100$ in some cases.

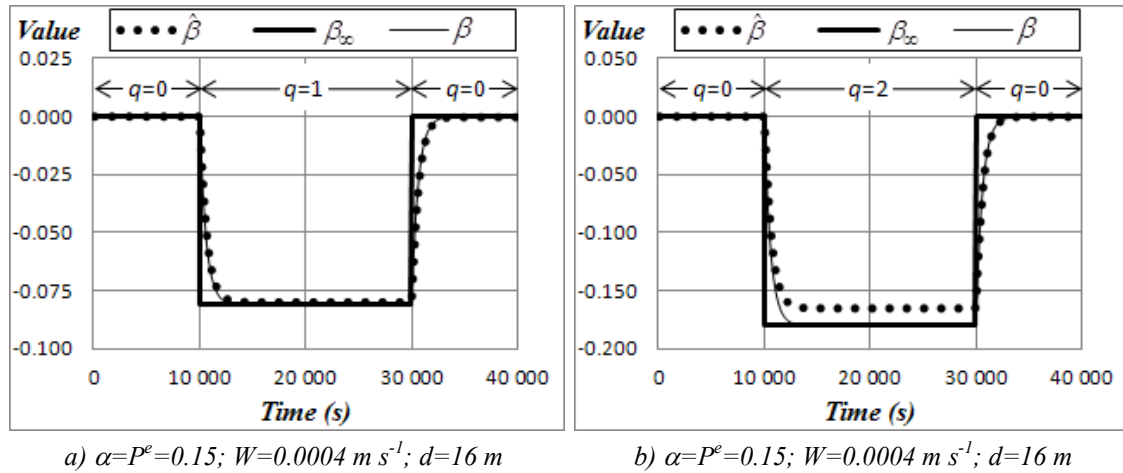
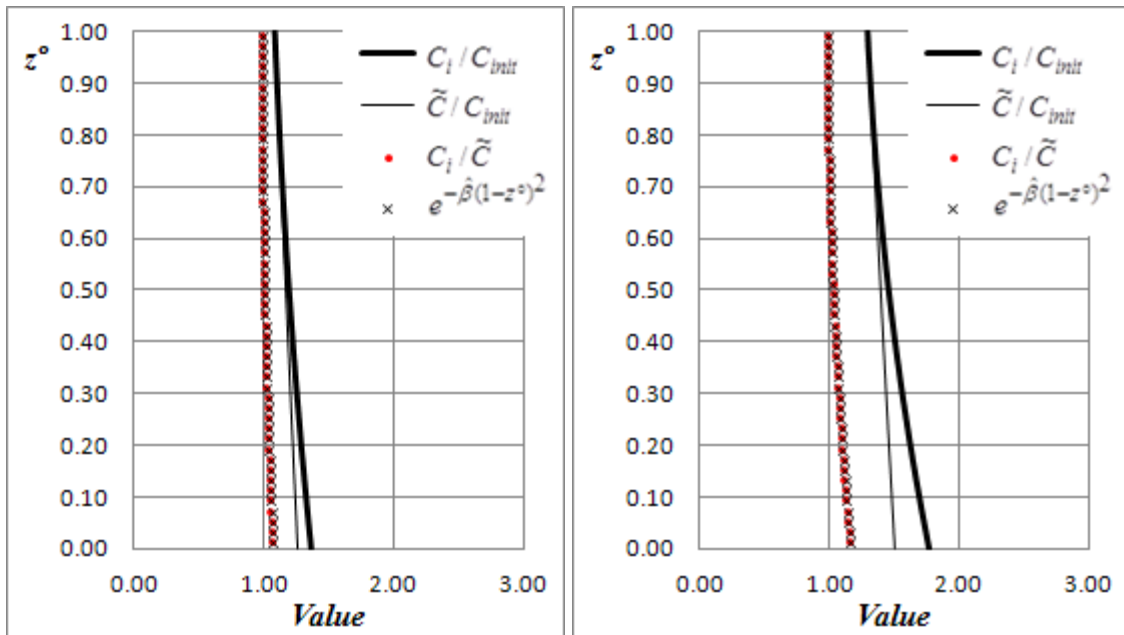


Figure 12. Results from 1DV numerical tests in unsteady state with erosion represented by values of $\hat{\beta}$. Evolution of $\beta_\infty(q, \alpha)$ according to its adjusted law, and variation of β according to the phenomenological model defined by equation (31) resolved by the predictor-corrector method of Runge-Kutta.

4.2.3 Simulations in unsteady state with erosion and deposition

Results obtained from 1DV modelling corresponding to the vertical dynamic of the suspended sediments in unsteady state with erosion and deposition, are presented in this section.



a) $\alpha=P^e=0.15; q=1; W=0.0004 \text{ m s}^{-1}; d=16 \text{ m}$ b) $\alpha=P^e=0.15; q=2; W=0.0004 \text{ m s}^{-1}; d=16 \text{ m}$

Figure 13. Results from 1DV numerical tests in unsteady state with erosion represented by an instantaneous profile of C_i/C_{init} . Instantaneous profile of \tilde{C}/C_{init} according to the phenomenological model without erosion or deposition. Ratio C_i/\tilde{C} and function $\hat{G}(z^o) = \exp(-\hat{\beta}(1-z^o)^2)$ adjusted from this ratio.

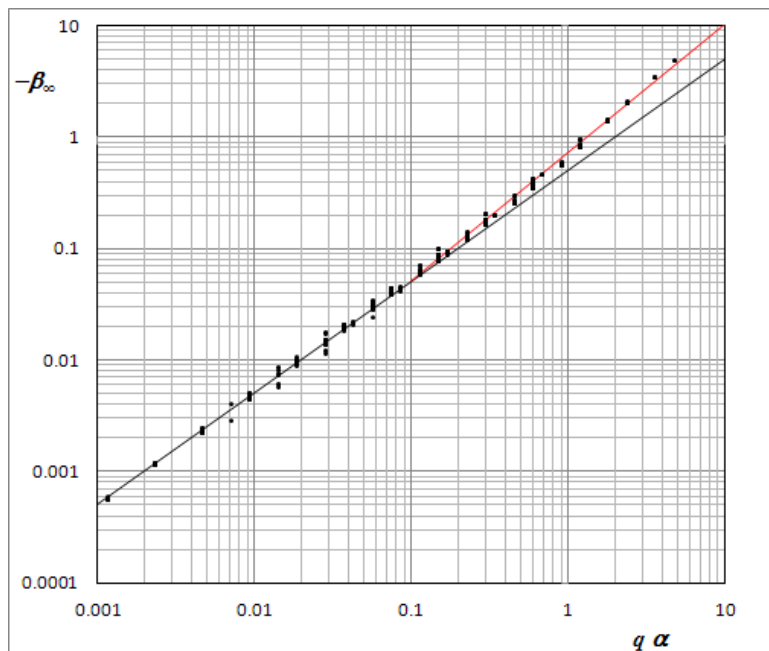


Figure 14. Values of $-\beta_\infty$ as a function of $p \times \alpha$ (596 experimental points). The black line corresponds to $\beta_\infty = -0.5(q\alpha)$, and the red line to the adjusted law for values of $q\alpha$ greater than 0.10 (see equation 35).

These results are compared with those obtained with the phenomenological model developed in this paper. The results of two simulations are described below. These simulations are referred to as Case 1 and Case 2.

The values of the variables of the problem relating to Case 1 are summarized in Table 1. As a consequence of the imposed values in this simulation, the dimensionless number ($U_{c-moy} \times T/d$) is relatively high, so that in the absence of deposition and erosion phenomena, sedimentary regimes would be nearly steady (see equation 25).

Results from 1DV model show, in line with those obtained from the phenomenological model (see Figure 15), that its non-dimensional parameters are nearly steady. It is observed that at every time α and β parameters are close of their respective α_∞ and β_∞ terminal values.

During the intervals of time when the vertical profile of the concentration is not affected by sediment exchanges between the bed and flow (erosion and deposition), the $\hat{\alpha}$ signal obtained from results of the numerical 1DV modelling is well approached by the signal $\alpha = \tilde{\alpha}$ of phenomenological models.

In the presence of deposition and erosion phenomena, signals α and $\hat{\alpha}$ diverge, which is due to a change of the shape of the vertical concentration profile with respect to its shape without deposition or erosion.

During the periods when the sediment dynamics is affected by erosion or deposition, a modification of the shape of the vertical concentration profile is controlled by parameter β . The very good agreement observed between β and $\hat{\beta}$ implies that the accuracy associated with phenomenological model results is excellent in this test-case.

In order to characterize a bulk accuracy of the phenomenological model, the relative errors at the bottom $e(z^\circ=0)$ are calculated as follows:

$$e(z^\circ = 0) = \frac{C(z^\circ = 0)}{C_i(z^\circ = 0)} - 1 = \frac{C_R \exp(-\beta)}{C_{i=1-\frac{1}{2}}(z^\circ = 0)} - 1 = \frac{C_R \exp(-\beta)}{1.5 C_{i=1} - 0.5 C_{i=2}} - 1 \quad (37)$$

Knowing that the vertical mean concentration is given by:

$$\bar{C} = \int_0^1 C_i dz^\circ \approx \int_0^1 C dz^\circ = \int_0^1 C_R \exp(-\alpha z^\circ) \exp(-\beta(1-z^\circ)^2) dz^\circ \quad (38)$$

The value of C_R is evaluated by:

$$C_R = \frac{\sum_{i=1}^N C_i \Delta z^\circ}{\sum_{i=1}^N \exp(-\alpha z_i^\circ) \exp(-\beta(1-z_i^\circ)^2) \Delta z^\circ} \quad (39)$$

It is observed that the signal of $e(0)$ contains moderate peak values associated with sudden beginning and end of erosion and deposition phenomena. Moreover, calculations show that the maximum values of $|e(z^\circ=0)|$ is less than 0.006, which confirms the very good accuracy accompanying the phenomenological model results in this case.

Table 1. Values of the problem variables defining Case 1 studied.

Variable	Symbol and value
Depth	$d = 2.00 \text{ m}$
Settling velocity	$W = 0.0002 \text{ m s}^{-1}$
Mean value of the shear velocity	$U_{c\text{-moy}} = 0.04 \text{ m s}^{-1}$
Signal period U_c	$T = 22320 \text{ s}$
Relative amplitude of the signal U_c	$Ampl=0.80$
Critical shear velocity for deposition	$U_c \text{ (critical for deposition)} = 0.50 \times U_{c\text{-moy}}$
Parameter of the Krone's deposition law	$p = 0.50$
Critical shear velocity for erosion	$U_c \text{ (critical for erosion)} = 1.70 \times U_{c\text{-moy}}$
Non dimensional effective erosion rate	$E^{ef} / (W \times \overline{C_{init}}) = 1.00$

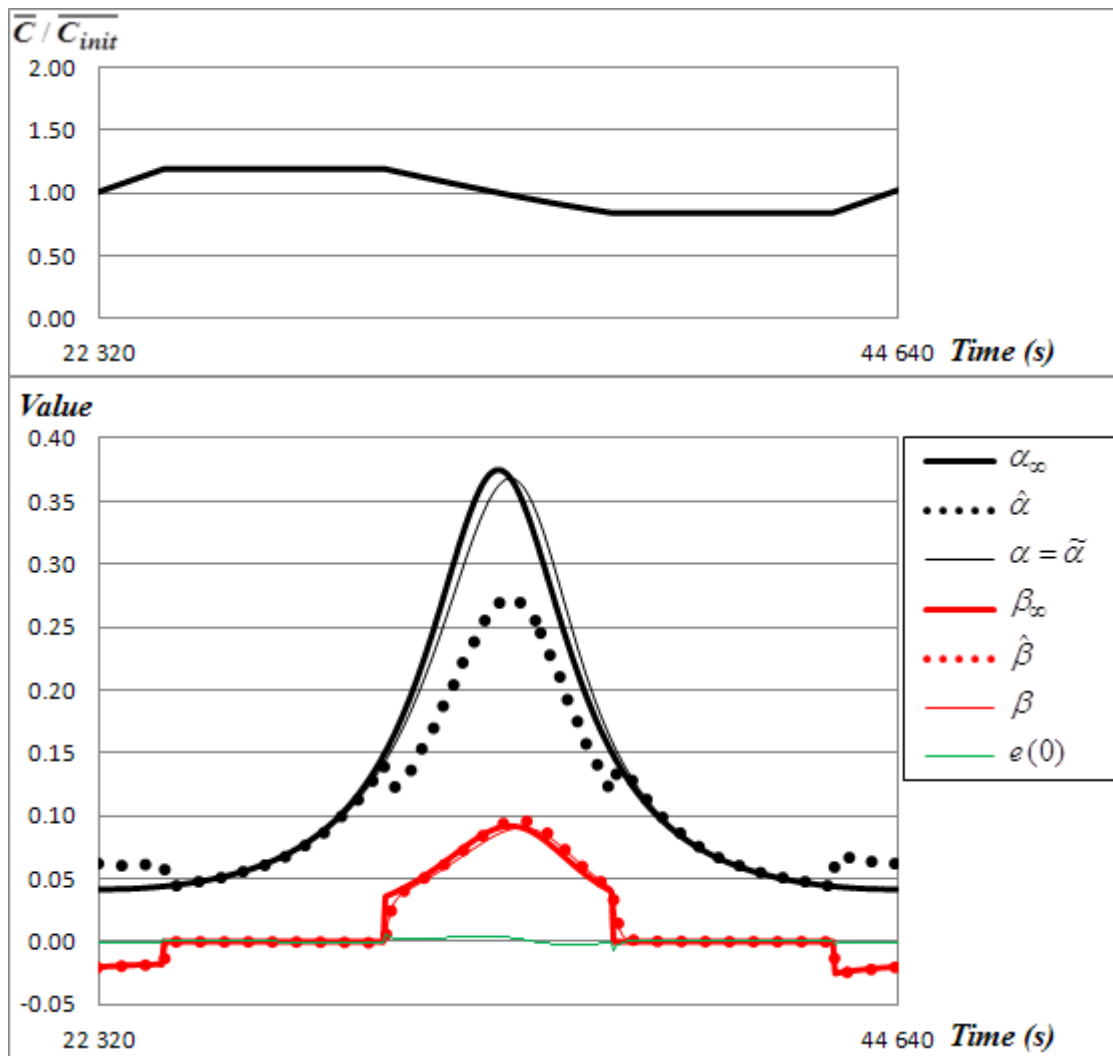


Figure 15. Results from models corresponding to Case 1, defined by the variable values gathered in table 1. This figure shows the time variations of the vertical mean concentrations and non-dimensional parameters of the phenomenological model describing the vertical suspended matter profiles.

The variable values connected with Case 2 are summarized in table 2 and the corresponding results are shown in Figure 16. It is found that α and α_∞ values are different as a rule, although both values are almost identical for low values of $\alpha_\infty = P^e$. The values of β are close to those of β_∞ during erosion phases that coincide with a low value of P^e , so that during periods of deposition, when P^e reaches its maximum values, the magnitudes of β and β_∞ are generally different.

In short, in this Case 2, the non-dimensional parameters of the phenomenological models approach their theoretical terminal values when P^e is small. That occurs for high values of U_c , which is the magnitude controlling the vertical sediment transfers associated with turbulence.

Extreme observed values of $e(0)$ are larger than in Case 1. Indeed, the absolute relative error reaches a maximum value of 0.10, which, for us, seems well acceptable.

Figure 17 shows vertical profiles of the concentration divided by the initial concentration of the test. Four sequences of profiles are shown, corresponding to four observation windows. The instants t_o of these windows correspond to:

- The beginning of deposition period.
- The end of deposition period.
- The beginning of erosion period.
- The end of erosion period.

In a general way, there is a very good agreement between the numerical results from the 1DV theoretical model and those from the phenomenological model. In all studied cases, a good convergence of the last one must be pointed out, although, during the period following the beginning of the deposition, a slight delay for the convergence near the bottom is found.

Table 2. Values of the problem variables defining Case 2 studied.

Variable	Symbol and value
Depth	$d = 8.00 \text{ m}$
Settling velocity	$W = 0.0012 \text{ m s}^{-1}$
Mean value of the shear velocity	$U_{c\text{-moy}} = 0.04 \text{ m s}^{-1}$
Signal period U_c	$T = 22320 \text{ s}$
Relative amplitude of the signal U_c	$Ampl = 0.80$
Critical shear velocity for deposition	$U_c \text{ (critical for deposition)} = 0.50 \times U_{c\text{-moy}}$
Parameter of the Krone's deposition law	$p = 1.00$
Critical shear velocity for erosion	$U_c \text{ (critical for erosion)} = 1.70 \times U_{c\text{-moy}}$
Non dimensional effective erosion rate	$E^{ef} / (W \times \overline{C_{init}}) = 2.50$

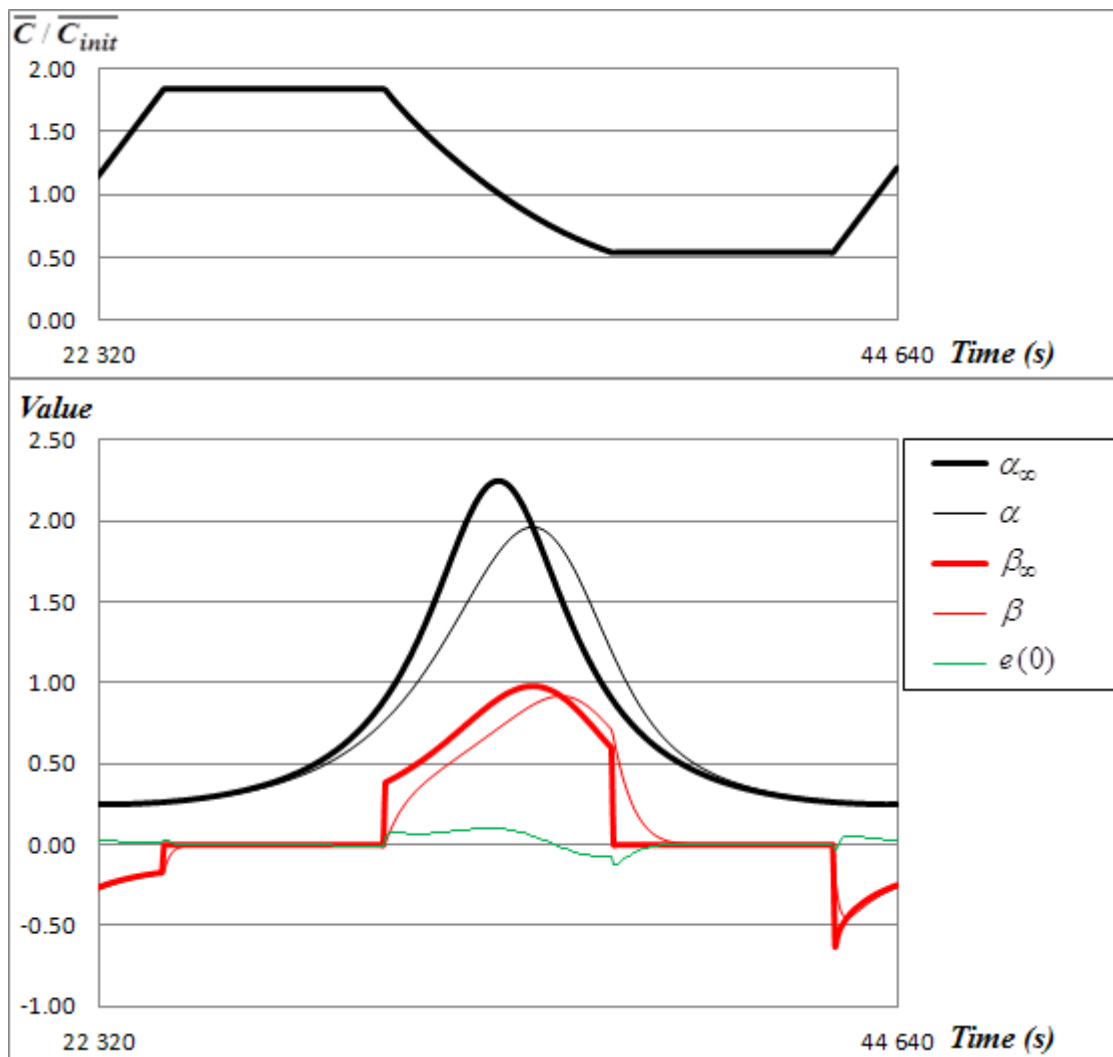


Figure 16. Results from models corresponding to Case 2, defined by the variable values gathered in table 2. This figure shows the time variations of the vertical mean concentrations and non-dimensional parameters of the phenomenological model describing the vertical suspended matter profiles.

5. Synthesis of the phenomenological model describing convection and diffusion of suspended matter

In the open surface flows studied in this paper, the suspended sediments are transported horizontally by the current. In these conditions, the phenomenological models developed for the parameters alpha and beta can be applied only if the sediments are followed in their horizontal movements. In Euler coordinates, that implies a need to include horizontal convection terms in the model equations.

Description non stationnaire de la distribution verticale des sédiments transportés en suspension par les écoulements à surface libre, en présence de dépôt et d'érosion : 9.83

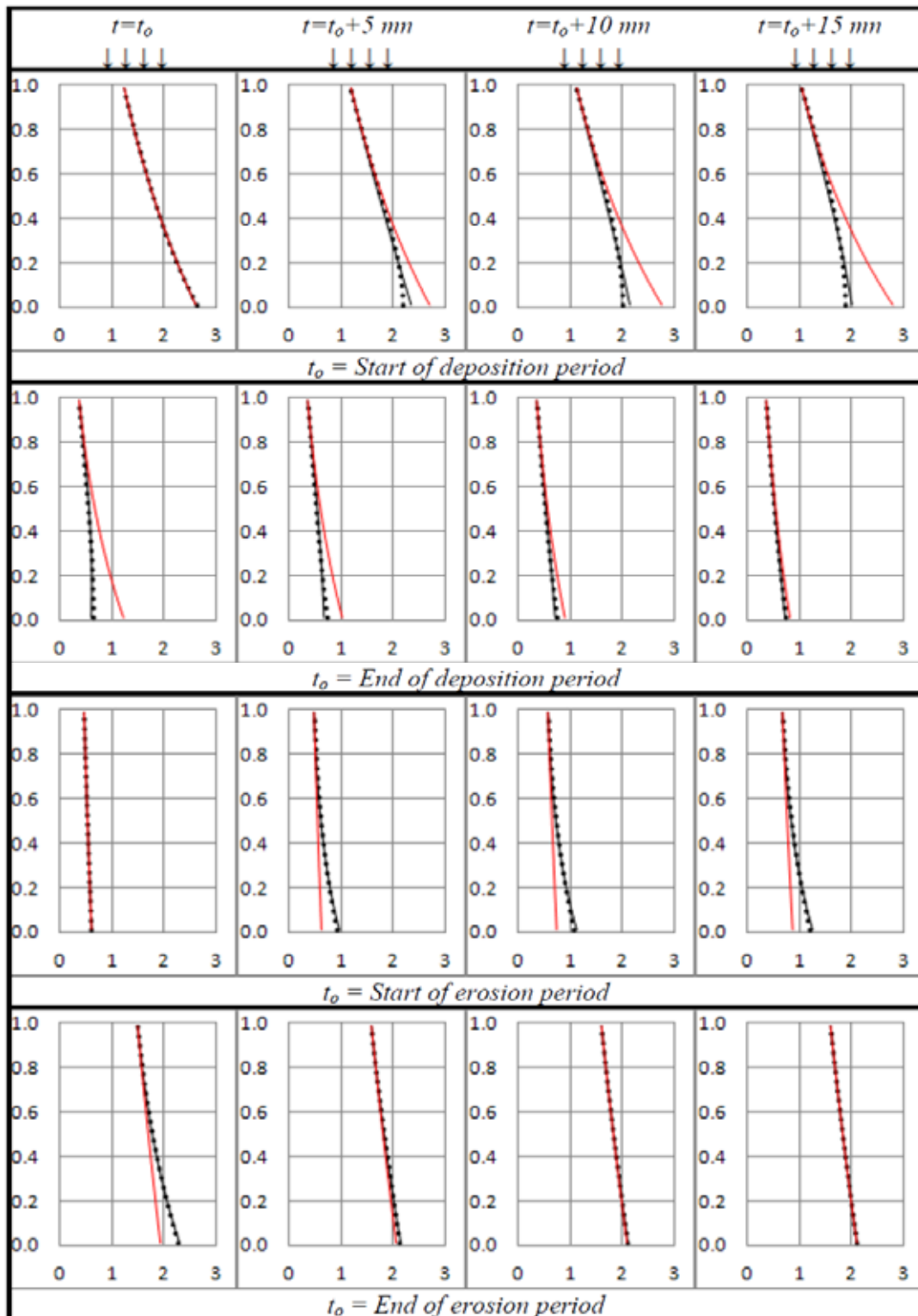


Figure 17. Concentrations divided by the initial concentration in the X-axis as a function of z° in the Y-axis. Dotted black line: numerical results from the IDV model. Black line: results from the phenomenological model. Red line: exponential law with alpha as unique non-dimensional parameter.

The final equations used in the 2DH transport model of suspended sediments by a flow are presented thereafter. First, the equation governing variations of the vertical mean concentration \bar{C} :

$$\frac{\partial \bar{C}}{\partial t} + \bar{V}_x \frac{\partial \bar{C}}{\partial x} + \bar{V}_y \frac{\partial \bar{C}}{\partial y} = \frac{\partial}{\partial x} \left(\bar{K}_x \frac{\partial \bar{C}}{\partial x} \right) + \frac{\partial}{\partial y} \left(\bar{K}_y \frac{\partial \bar{C}}{\partial y} \right) + \frac{E^{ef} - D^{ef}}{d} \quad (40)$$

where \bar{V}_x and \bar{V}_y are the components of the vertical mean velocity of the flow in the Ox and Oy directions respectively.

The vertical profile of the concentration is described by equation 27, given below:

$$C(z^\circ) = C_R \exp(-\alpha z^\circ) \exp(-\beta(1 - z^\circ)^2)$$

From equation 38, the reference concentration of the profile C_R is connected to \bar{C} by:

$$\bar{C} = C_R \int_0^1 \exp(-\alpha z^\circ) \exp(-\beta(1 - z^\circ)^2) dz^\circ$$

The bottom concentration C_0 , whose value is necessary to evaluate the effective deposition rate D^{ef} , is linked to C_R by:

$$C_0 = C_R \exp(-\beta)$$

The parameter $\alpha = \tilde{\alpha}$, in accordance with equation 24, and taking into account the horizontal convection, is governed by:

$$\frac{\partial \alpha}{\partial t} + \bar{V}_x \frac{\partial \alpha}{\partial x} + \bar{V}_y \frac{\partial \alpha}{\partial y} = c_\alpha \frac{U_c}{d} (\alpha_\infty - \alpha) \quad (40A)$$

where $\alpha_\infty = P^e$ is the terminal steady state value of the parameter α and $c_\alpha \approx 0.667$ is a coefficient of the model. By including horizontal convection in equation 31, governing parameter β , it becomes:

$$\frac{\partial \beta}{\partial t} + \bar{V}_x \frac{\partial \beta}{\partial x} + \bar{V}_y \frac{\partial \beta}{\partial y} = c_\beta \frac{U_c}{d} (\beta_\infty - \beta) \quad (40B)$$

where β_∞ is the terminal steady state value of parameter β , which depends on the sediment exchanges between the bed and the water column. These exchanges are parameterized by D^{ef} and E^{ef} .

In the case of effective deposition ($D^{ef} > 0; E^{ef} = 0$):

$$\beta_\infty = 0.50 p \alpha \quad , \text{and} : c_\beta = 0.667 + 0.3 \times \beta$$

In the case of effective erosion ($D^{ef} = 0; E^{ef} > 0$):

$$\beta_\infty = \begin{cases} -0.50 \times (q\alpha) & , \text{if} : q\alpha < 0.10 \\ -0.72 \times (q\alpha)^{1.15} & , \text{if} : q\alpha > 0.10 \end{cases} \quad , \text{et} : c_\beta = 0.667$$

In the case of nil effective exchanges between the bed and the flow ($D^{ef} = 0; E^{ef} = 0$):

$$\beta_\infty = 0 \quad , \text{and} : c_\beta = 0.667$$

5.1 Two equations vertical convective-diffusive model

This model should be used when α and β are generally different of α_∞ and of β_∞ , respectively.

If the hydrodynamic actions parameterized by $|U_c|$ have a periodicity T , this case corresponds to a dimensionless number $(U_{c-moy} \times T/d) \ll 500$. The non-dimensional parameters of the model must be simulated by equations 40A and 40B. The results are then reliable at all times.

5.2 One equation vertical convective-diffusive model

In some problems, at any moment $\beta \approx \beta_\infty$, while in general $\alpha \neq \alpha_\infty$. In these problems $\beta = \beta_\infty$ must be retained, but since $\alpha(t)$ is delayed compared to $\alpha_\infty(t)$, it must be simulated by equation 40A. The fact of retaining $\beta = \beta_\infty$ can induce some significant errors over short periods of time following the end of the depositional and erosional periods (see Figures 15 and 16). This case corresponds to $(U_{c-moy} \times T/d) \approx 500$

5.3 Zero equation vertical convective-diffusive model

In this case, the stationarity of the parameters α and β is observed. Then, $\alpha = \alpha_\infty$, and $\beta = \beta_\infty$ can be retained. This case corresponds to $(U_{c-moy} \times T/d) > \sim 500$ with very short or no periods, with low values of U_c . The results for C_0/\bar{C} are then very close to those calculated by the formulation of TEETER (1986), (equation 14), and practically identical for values of p close to 1.

6. Conclusions

The study of the vertical profile shapes of the suspended sediment concentrations allow to draw two general conclusions, non-dependent on the phenomenological model developed in this paper:

- In steady sedimentary state, analytical or numerical solutions of the equations governing the problem allow to describe C/C_0 profiles by a function $F(z^\circ; \alpha_\infty)$ defining the general equation of these profiles, where α_∞ is a non-dimensional parameter which depends on the W/U_c ratio.

For unsteady state, when conditions without erosion or deposition are imposed in the modelling, at any time the C/C_0 profiles converge towards $F(z^\circ; \alpha_\infty)$. Although the real convergence is faster at the bottom and surface than over the rest of the water column, in most cases C/C_0 profiles are fairly well modelled by the same function $F(z^\circ; \alpha)$, with the value of the parameter α always tending towards the instantaneous value of α_∞ . According to modelling, the only significant deviation from this general equation of the C/C_0 profile is observed when the phase shift between the signals $\alpha(t)$ and $\alpha_\infty(t)$ is very important. That occurs for values of U_c which tend towards zero ($(W/U_c) \rightarrow \infty$), for which, compared to the general equation of the profile C/C_0 , an over-accumulation of sediment in the layers of the water column located near the bottom is caused by the 1DV transport equation governing the vertical dynamics of the suspended matters. This over-accumulation disappears when the values of U_c rise

again. This deviation from the general equation of the profile is largely an artifact of the modelling, because, in these conditions, deposition must occur.

- With deposition or erosion, if the independent variables of the problem (U_c , W et d) are constant, and if the sediment exchanges with the bed are proportional to the settling velocity multiplied by the bottom concentration (constant parameters p and q), the 1DV modelling shows that the profile of the $C/F(z^\circ; \alpha)$ ratio always tends towards a terminal shape, and remains similar thereafter.

If these conditions persist long enough, a terminal form defined by a function $G(z^\circ; \beta_\infty)$ is reached. Then, a stationarity of the parameter β_∞ is observed, so that the C -profiles can be modelled by a function $C_R \times F(z^\circ; \alpha) \times G(z^\circ; \beta_\infty)$, where $F(z^\circ; \alpha)$ is the function describing the C/C_0 profile for unsteady state without deposition or erosion. If stationarity is not reached for β , the vertical profile of C is not exactly described by $C_R \times F(z^\circ; \alpha) \times G(z^\circ; \beta)$, but this expression is, however, a satisfactory approach.

The main numerical results of this study were obtained with a turbulent diffusivity coefficient K_z , invariant with z . This same approach can be applied when K_z varies with z , which implies a possible modification of functions $F(z^\circ; \alpha)$ and $G(z^\circ; \beta)$ (see Appendix 1).

When K_z is constant over all the water column, the functions used are $F(z^\circ; \alpha) = \exp(-\alpha z^\circ)$ and $G(z^\circ; \beta) = \exp(-\beta(1-z^\circ)^2)$. The terminal value of the parameter α is $\alpha_\infty = P^e$, and that of β is either a function $\beta_\infty(p, \alpha) = 0.5 p \alpha$, in case of deposition or a function $\beta_\infty(q, \alpha)$ in case of erosion (equation 35). According to the phenomenological model developed in this article, the variations of α and β , can be simulated by equations 40A and 40B, respectively. In this model, α and β converge uniformly over the entire water column towards α_∞ and β_∞ , respectively, which is an approximation of the problem because the real convergence appears to be faster at the bottom and surface than over the rest of the water column.

The best validation of the phenomenological model is its proven ability to reproduce the vertical dynamics of suspended sediments and to provide results which are very similar to those obtained from a numerical solution of a 1DV theoretical equation with a discretization of the water column that uses at least 50 layers.

In applications to real cases, errors linked to the phenomenological model results are acceptable if erosion and deposition are set correctly. However, with depositional conditions, if $p=0$ is imposed, the relative errors in the modelling results reach a value of 0.40, when $(U_{c-moy} \times T/d) \approx 7$ and $P^e = 12$ (see Figure 5b). This error is largely a bias of modelling because this case is extreme, with very marked depositional conditions, so that $p=0$ is unrealistic.

Insofar as the phenomenological model approaches the theoretical solution of the problem, the following two conclusions on sedimentary behaviour reflect a reality, at least on average, over the water column:

- In agreement with this model, the value of α always tends towards P^e . Without erosion or deposition, when $\alpha \approx P^e$ the vertical profile of the concentration is under conditions close to equilibrium between settling and convection, over the entire water column. If the independent variables (U_c , W and d) remain constant, the time required to achieve this equilibrium can be characterized by a time constant $\tau_\alpha = d/(c_\alpha \times U_c)$, so that after a time $t = 4.6 \times \tau_\alpha$, we get: $(\alpha_\infty - \alpha) = (\alpha_\infty - \alpha_{init})/100$, where α_{init} is the initial value of this parameter (at $t=0$).

This expression of the time constant is justified by the fact that to achieve the equilibrium conditions, the suspended sediments must be redistributed over the entire height d of the water column, and the rate of the vertical transfers of sediment by mixing is controlled by U_c .

- The non-dimensional parameter β of the model is associated with the effects of the sediment exchanges between the bed and the flow, on the vertical concentration profile. After a depositional or erosional period, when the sediment exchanges at the bottom stop, the value of β tends to zero as suspended sediments redistribute over the water column, approaching thus sedimentary states, either steady or unsteady, without deposition or erosion. When the independent variables of the problem are constant and p or q remains constant, in case of deposition or erosion, respectively, the time required for β to reach its final value β_∞ is characterized by a time constant $\tau_\beta = d/(c_\beta \times U_c)$.

It should be noted that this research was developed specifically for applications on fine sediments, but the presented methods and results can be applied to all types of material transported in suspension by any stream, on condition that the variables of the problem are well parameterized.

For the final conclusion, we can say that the phenomenological model developed in the context of this paper to describe the vertical profile of the concentrations in hydrosedimentary 2DH models can significantly improve the accuracy and quality of information that can be obtained from modelling.

7 Appendices

7.1 Appendices 1: Analytical solutions for the vertical profile of suspended matter concentration in a flow

If the suspended sediment profile is in equilibrium (without erosion or deposition) integration of equation 8 leads to the generalized Rouse-Vanoni law for the vertical steady state distribution of the concentration (ORTON & KINEKE, 2001; SANCHEZ *et al.*, 2005), that is:

$$C(z)|_{steady-state} = C_0 \exp\left(-\int_0^z \frac{W}{K_z} dz\right)$$

The solution of this equation depends on the formulations chosen to describe W and K_z . In this paper, W and K_z are studied as constant magnitudes, so, in steady state, concentration is given by equation 10.

Another widely known solution for concentration in steady state, which is due to ROUSE (1937), assumes W invariant with z , and K_z described by:

$$K_z = \kappa U_c z (1 - z^0)$$

The corresponding solution, which is valid for $z \geq a$, is obtained since:

$$\int_a^z \frac{dz}{K_z} = \frac{1}{\kappa U_c} \ln \left[\frac{z(d-a)}{a(d-z)} \right]$$

therefore we can write:

$$C(z)|_{steady-state} = C_a \exp \left(- \frac{W}{\kappa U_c} \ln \left[\frac{z(d-a)}{a(d-z)} \right] \right) = C_a \left[\frac{a(d-z)}{z(d-a)} \right]^{W/(\kappa U_c)}$$

where C_a is the reference concentration near the bed at a level $z=a$ from the bottom. The evaluation of C_a/\bar{C} ratio from this equation is very sensitive to the value used for a , which, according to some authors, is equal to $0.05 \times d$, but for other authors, is in the same order of magnitude as the bed roughness.

In a more general way, if K_z is a function of z , and W depends on the local concentration C , in accordance with a power law which can be written as follows:

$$W = W_0 \left(\frac{C}{C_0} \right)^{1/r}$$

where W_0 is the value of settling velocity associated with the concentration at the bottom C_0 , and r is a constant, then, the vertical profile of the concentration is described by:

$$C(z)|_{steady-state} = C_0 \left(\frac{\lambda_0}{\lambda_z} \right)^r$$

with $\lambda_0 = r/W_0$, and λ_z which is given by:

$$\lambda_z = \lambda_0 + \int_0^z \frac{dz}{K_z}$$

These last three equations remain valid if, from a viewpoint similar to that adopted to statistically classify the diameter of sand grains in granulometric studies, the settling velocity is described according to a gamma distribution of parameters r and λ_z (SANCHEZ, 2006).

7.2 Appendices 2: Relation between the bottom concentration and the vertical mean concentration as a function of the non-dimensional parameters of the phenomenological model describing the suspended matter vertical profile

From equations 27 and 38 can be written:

$$\frac{C_0}{\bar{C}} = \frac{\exp(-\beta)}{\int_0^1 \exp(-\alpha z^\circ) \exp(-\beta(1-z^\circ)^2) dz^\circ}$$

This expression admits an analytical solution for $\beta=0$ and can be evaluated by using integral tables of the normal Gaussian distribution when $\beta=0.5\alpha$. However, in a general case, this equation must be numerically integrated as follows:

$$\frac{C_0}{\bar{C}} = \frac{\exp(-\beta)}{\sum_{i=1}^N \exp(-\alpha z_i^\circ) \exp(-\beta(1-z_i^\circ)^2) \Delta z^\circ}$$

Figure 18 shows C_0/\bar{C} as a function of β/α for some values of α .

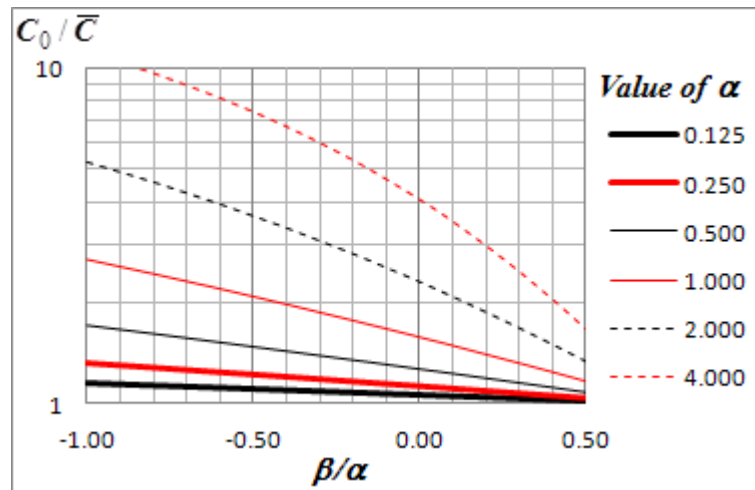


Figure 18. Variation of C_0/\bar{C} as a function of β/α for some values of α according to the phenomenological model describing the suspended matter vertical profile, which has been carried out in this paper.

8. References

- BELINSKY M., RUBIN H., AGNON Y., KIT E., ATKINSON J.F. (2005). *Characteristics of resuspension, settling and diffusion of particulate matter in a water column*. Environmental. Fluid Mechanics, Vol. 5, pp 415-441. doi:10.1007/s10652-004-7302-3
- KRONE R.B. (1986). *The significance of aggregate properties to transport processes*. In A.J. Mehta (Ed.), *Estuarine cohesive sediment dynamics*, Coastal and estuarine studies n° 14 (pp. 66–84). Springer, Berlin. doi:10.1007/978-1-4612-4936-8_4

LUMBORG U., WINDELIN A. (2003). *Hydrography and cohesive sediment modelling: application to Rømø Dyb tidal area*. Journal of Marine Systems, Vol. 38, pp 287–303. doi:10.1016/S0924-7963(02)00247-6

MEHTA A.J. (1986). *Characterization of cohesive sediment properties and transport processes in estuaries*. In A.J. Mehta (Ed.), Estuarine cohesive sediment dynamics, Coastal and estuarine studies n° 14 (pp. 290–325). Springer, Berlin.

doi:10.1007/978-1-4612-4936-8_15

ORTON P.M., KINEKE G.C. (2001). *Comparing calculated and observed vertical suspended-sediment distributions from a Hudson River estuary turbidity maximum*. Estuarine, Coastal and Shelf Science, Vol. 52, pp 401–410. doi:10.1006/ecss.2000.0747

ROUSE H. (1937). *Modern conceptions of the mechanics of fluid turbulence*. Transactions of the American Society of Civil Engineers, Vol. 102, pp 463–541.

SANCHEZ M. (2006). *Settling velocity of the suspended sediment in three high-energy environments*. Ocean Engineering, Vol. 33 (5-6), pp 665–678.

doi:10.1016/j.oceaneng.2005.05.009

SANCHEZ M., GRIMIGNI P., DELANOË Y. (2005). *Steady-state vertical distribution of cohesive sediments in a flow*. Comptes Rendus Geoscience, Vol. 337, pp 357–365.

doi:10.1016/j.crte.2004.10.020

TEETER A.M. (1986). *Vertical transport in fine-grained suspension and newly-deposited sediment*. In A.J. Mehta (Ed.), Estuarine cohesive sediment dynamics, Coastal and estuarine studies n° 14 (pp. 170–191). Springer, Berlin. doi:10.1007/978-1-4612-4936-8_9

Complementary note about the paper indexed DOI:10.5150/revue-paralia.2013.009

Note received 19 October 2015, accepted 6 November 2015, available online 9 November 2015.

Additional numerical tests of which some results has been published by SANCHEZ (2014), show that in case of erosion the parameter β_∞ can be linked to $q\alpha$ by one unique expression satisfying bottom border conditions associated with solid exchanges between the bed and the flow:

$$\beta_\infty = -0,50 q\alpha \quad , \text{ for every value of } q\alpha \quad (\text{Eq. 35 modified})$$

In case of deposition ($D^{ef} > 0$) in this paper the coefficient c_β was linked to β by equation 32, on the basis of results obtained from numerical simulations carried out with $\beta = \beta_\infty$. When $\beta \neq \beta_\infty$ results are improved if the c_β coefficient is related to β_∞ through equation 32 modified as follows (see SANCHEZ, 2014):

$$c_\beta = \begin{cases} 0,667 + 0,3 \times \beta_\infty & , \text{ if: } D^{ef} > 0 \\ 0,667 & , \text{ if: } D^{ef} = 0 \end{cases} \quad (\text{Eq. 32 modified})$$

Référence bibliographique :

SANCHEZ M. (2014). *Distribution non stationnaire des matières en suspension dans une couche limite oscillant à haute fréquence*. XIII^{ème} Journées Nationales Génie Côtier – Génie Civil, Dunkerque, pp 495-504. doi:10.5150/jngcgc.2014.054